ORIGINAL PAPER

# Arsenic interactions with a fullerene-like BN cage in the vacuum and aqueous phase

**Javad Beheshtian · Ali Ahmadi Peyghan · Zargham Bagheri**

**Abstract** Adsorption of arsenic ions, As (III and V), on the surface of fullerene-like $B_{12}N_{12}$ cage has been explored in vacuum and aqueous phase using density functional theory in terms of Gibbs free energies, enthalpies, geometry, and density of state analysis. It was found that these ions can be strongly chemisorbed on the surface of the cluster in both vacuum and aqueous phase, resulting in significant changes in its electronic properties so that the cluster transforms from a semi-insulator to a semiconductor. The solvent significantly affects the geometry parameters and electronic properties of the As/$B_{12}N_{12}$ complexes and the interaction between components is considerably weaker in the aqueous phase than that in the vacuum.

**Keywords** *Ab initio* · B3LYP · DFT · Fullerene-like cage · Sensor

## Introduction

Arsenic is one of the most toxic elements distributed in the natural environment, rocks, natural waters, soils, and

J. Beheshtian
Department of Chemistry, Shahid Rajaee Teacher Training University, P.O. Box: 16875-163, Tehran, Iran

A. A. Peyghan (✉)
Young Researchers Club, Islamic Azad University, Islamshahr Branch, Tehran, Iran
e-mail: ahmadi.iau@gmail.com

Z. Bagheri
Physics group, Science Department, Islamic Azad University, Islamshahr Branch , P.O. Box: 33135-369, Islamshahr, Tehran, Iran

organisms. Arsenic pollution is growing seriously with the industry development of mining, leather, ceramics, etc. This toxic element can be found in several oxidation states (−3, 0, +3, and +5) in the natural environment. In natural water, inorganic arsenic is mostly found as trivalent arsenite or pentavalent arsenate. Since the arsenite has higher affinity for protein than the arsenate, it is 25–60 times more toxic and it has been reported that it is more mobile in the environment [1]. Arsenic removal methods include ion-exchange, adsorption, chemical precipitation, biological methods, etc. The adsorption process has been extensively used due to good effect, easy operation, and other advantages. Iron minerals, activated carbon, and zeolites are traditional adsorbents for the arsenic separation [2].

An ideal adsorbent should have a suitable particle size or uniformly accessible pores, chemical stability, and high surface area. At the end of the twentieth century, development of nanotechnology has spanned the possibility of using a variety of adsorbents [3, 4]. Several reports have demonstrated a possible mechanism for adsorption of arsenic on different nano-adsorbents [5, 6]. During the last decade, fullerene-related materials have attracted great attention due to their unique physical and chemical properties [7–9]. $B_{12}N_{12}$ cage is one of the most interesting cases, due to having a structure based on decoration of truncated octahedrons in which all B vertices remain equivalent, as do all N vertices [10]. Oku et al. have synthesized the $B_{12}N_{12}$ cage, showing that these clusters consist of 4- and 6-membered rings (6-MR) of BN with the band gap energy of 5.1 eV [10]. Recently, we have shown that the $B_{12}N_{12}$ cage may be a potential sensor for CO, $NO_2$, and NO in the presence of $H_2$, $N_2$, and $CH_4$ molecules [11–13]. The main objective of the present research is to study the adsorption of arsenite and arsenate on the $B_{12}N_{12}$ cage in vacuum and aqueous media using density functional theory in terms of structural, energetic and electronic properties.

## Computational methods

Geometry optimizations and density of states (DOS) analysis were performed on a boron nitride cage of $B_{12}N_{12}$, and different As (III or V)/$B_{12}N_{12}$ complexes at the B3LYP/6-31G* level of theory as implemented in the GAMESS suite of program [14]. Vibration frequencies have also been calculated at the same level to confirm that all the stationary points correspond to true minima on the potential energy surface. The B3LYP density functional has been shown to reproduce experimental properties [15] and is commonly used for nanostructured materials [16–21]. It has been also demonstrated by Tomic et al. [22], that the B3LYP provides an efficient and robust basis for calculations of III–V semiconductors capable of reliably predicting both the ground state energies and the electronic structure. We have used the definition of the adsorption enthalpy ($\Delta H°$) for a cation on the $B_{12}N_{12}$ (at T=298.18 K and P=1 atm) as follows:

$$\Delta H° = H°_{complex} - H°_{cage} - H°_{As}, \tag{1}$$

where $H°_{complex}$ is the total energy of the complex (an adsorbed arsenic ion on the $B_{12}N_{12}$ surface), and $H°_{cage}$ and $H°_{As}$ are the total energies of the bare $B_{12}N_{12}$ cage and an As (III or V) ion, respectively. As is well known, a negative value of $\Delta H°$ corresponds to exothermic adsorption. Adsorption free energies ($\Delta G°$) have also been calculated similar to the $\Delta H°$, using corresponding data at the same condition. Solvation effects have been included through the use of the polarizable continuum model (PCM). A dielectric constant of 78.4 was used for water as the solvent. Gas-phase structures have been subsequently used as starting points for further geometry optimization in the PCM approach.

## Results and discussion

### The $B_{12}N_{12}$ properties

Optimized structure for the pristine $B_{12}N_{12}$, its DOS plot, and IR spectra (Fig. 1) are depicted in Fig. 1, in which two types of B-N bonds can be identified, one has been shared between two 6-MRs ($B_{66}$), and the other has been shared

between 4- and 6-MR ($B_{64}$). Calculated bond lengths are about $B_{66}$=1.439 and $B_{64}$=1.486 Å. The charge analysis using the Mulliken method indicates that about 0.44 $e$ charges are transferred from the boron atom to its neighboring nitrogen atoms within the sidewall, illuminating that the B-N bonds are partially ionic. The DOS plot shows that the cluster is a semi-insulator substance with the HOMO/LUMO energy gap ($E_g$) of 6.84 eV. As is seen from the IR spectra, there are no imaginary frequencies, indicating that the cluster is true minima on the potential energy surface. Calculated IR frequencies are found to be in the range of 323.9 to 1446.3 $cm^{-1}$ in the gas phase and 323.3 to 1427.5 $cm^{-1}$ in the aqueous medium.

### Adsorption of As ions on the $B_{12}N_{12}$ in the gas phase

First, we have explored the stable configurations (local minima) of As (III) ion on the sidewall of the $B_{12}N_{12}$ cage in the gas phase. To this end, the As (III) ion was initially placed on different sites including atop a B or N atom, bridge site of the $B_{66}$ or $B_{64}$ bond, and above the center of 6-MR or 4-MR. Ensuring that the most stable configuration has been achieved, the initial distance between the molecule and the cluster has been adjusted several times from 2.0 to 3.5 Å. Full structural relaxation, without any constraint, was then performed on each of the initial configurations. Finally, we have obtained only two stable structures with positive vibrational frequencies, as shown in Fig. 2 (configurations **A.3** and **B.3**). In the configuration **A.3**, the As (III) ion has been relaxed above the center of 6-MR so that its distance from N atoms is about 1.90–1.92 Å. The $\Delta H°$ and $\Delta G°$ values for this configuration are about −21.0 and −20.8 eV, respectively, showing the high strength nature of the interaction between the As ion and the cluster. A less negative value has been obtained for $\Delta G°$ in comparison with $\Delta H°$ which can be attributed to the entropic effect, i.e., the change of entropy during the adsorption process is positive.

The obtained results from the Mulliken population analysis show that the net charge on the adsorbed As ion is about 1.98 e which indicates that a quantity of 1.02 e charge has been transferred from the cluster to the ion. Calculated DOS shows that this phenomenon leads to decrement of $E_g$ to approximately half of its original value, so that the cluster

Fig. 1 Optimize structure of $B_{12}N_{12}$ cage, its DOS plot and IR spectrum
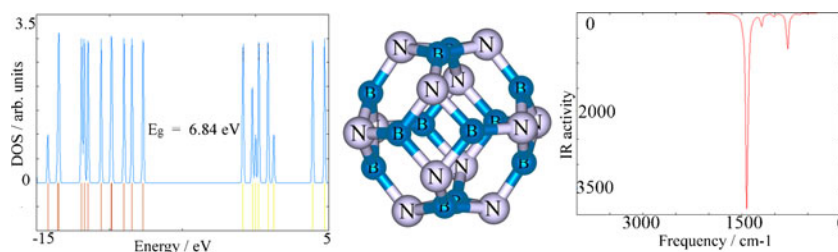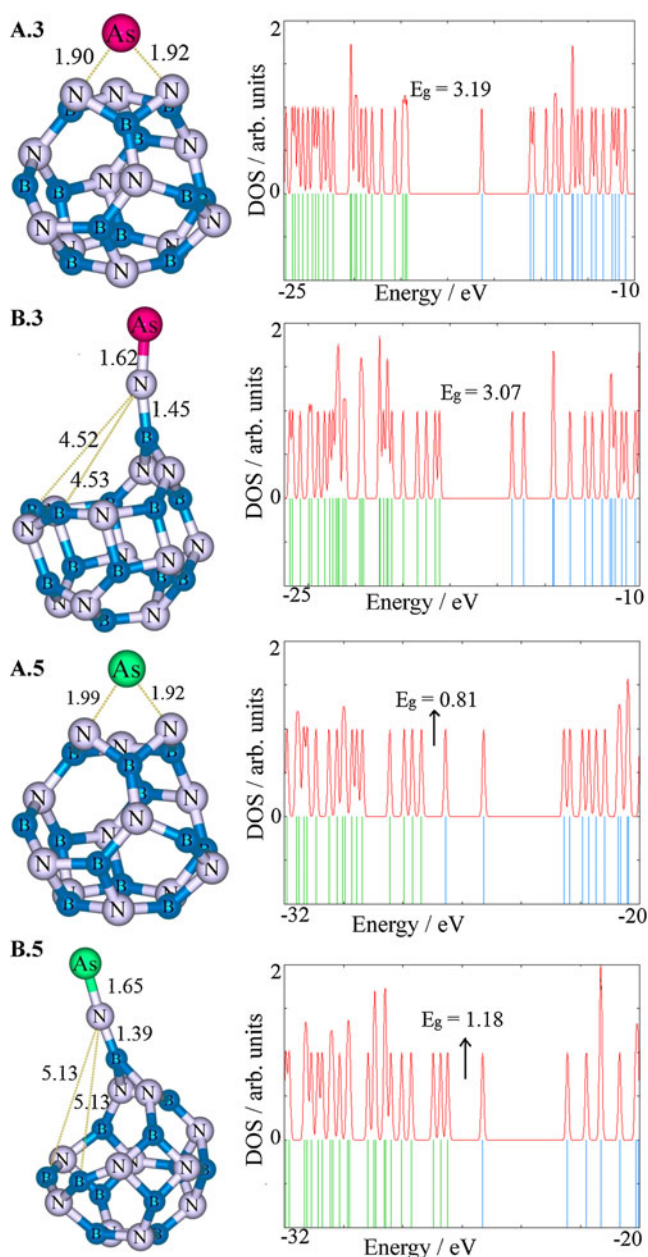
**Fig. 2** Geometry parameters of As/$B_{12}N_{12}$ complexes in vacuum and their density of state (DOS) plots. As (III) and (V) ions are shown in red and green, respectively. Distances are in Å

transforms from a semi-insulator with the $E_g$ of 6.84 eV to a semiconductor with the $E_g$ of 3.19 eV. This phenomenon is expected to bring about obvious change in the corresponding electrical conductivity because it is well known that the $E_g$ (or band gap in bulk materials) is a major factor determining the electrical conductivity of a material and there is a classic relation between them as follows [23]:

$$\sigma \propto \exp\left(\frac{-E_g}{2kT}\right), \tag{2}$$

where $\sigma$ is the electrical conductivity and $k$ is the Boltzmann's constant. According to this equation, smaller $E_g$ at a given temperature leads to higher electrical conductivity. However, the $E_g$ of the As/cluster complex is significantly reduced compared to that of the pristine cluster. Since the conductivity is exponentially correlated with the negative value of $E_g$, it is expected that it becomes larger with decreasing $E_g$. It demonstrates high sensitivity of the electronic properties of the $Al_{12}N_{12}$ toward the adsorption of the As ion.

The trend of As (III) adsorption on the $B_{12}N_{12}$ in configuration **B.3** is completely different from that in **A.3**. In the later configuration (Fig. 2), an As (III) has been strongly adsorbed on the N atom so that two adjacent N-B bonds have been completely broken and their distance has been reached to 4.52–4.53 Å, creating a window on the surface of the cluster. However, this phenomenon may be interesting because it is of great importance in small molecule insertion into the inner space of the fullerenes and nano-cages [1]. The $\Delta H°$ and $\Delta G°$ values for this configuration are found to be about −22.6 and −22.5 eV, respectively, which are slightly more negative than those of configuration **A.3**. The charge transfer and the change of electronic properties of the cluster are nearly similar to those of the **A.3** (Table 1 and Fig. 2).

The two obtained adsorption configurations (**A.5** and **B.5**, Fig. 2) for As (V) are approximately analogous to the corresponding As (III)/cluster complexes but the As (V) adsorption on the cluster is much stronger than the adsorption of As (III). Calculated values of $\Delta G°$ for **A.5** and **B.5** are about −86.9 and −98.9 eV along with charge transfers of 1.47 and 1.33 e, respectively, from the cluster to the As (V).

**Table 1** Calculated data for adsorption of As (III and V) ions on the $B_{12}N_{12}$ cage in vacuum. The energies are in eV

| System | $\Delta H°$ | $\Delta G°$ | $Q_T$ (e) | $E_{HOMO}$ | $E_{LUMO}$ | $E_g$ | [a]$\Delta E_g$(%) |
|---|---|---|---|---|---|---|---|
| $B_{12}N_{12}$ | – | – | – | −7.71 | −0.87 | 6.84 | – |
| A.3 | −21.0 | −20.8 | 1.98 | −19.74 | −16.55 | 3.19 | 53.4 |
| B.3 | −22.6 | −22.5 | 1.99 | −18.45 | −15.38 | 3.07 | 55.1 |
| A.5 | −87.1 | −86.9 | 3.57 | −27.37 | −26.56 | 0.81 | 88.2 |
| B.5 | −91.0 | −90.9 | 3.66 | −26.48 | −25.30 | 1.18 | 82.7 |

[a] The change of $E_g$ (HOMO/LUMO energy gap) of $B_{12}N_{12}$ upon the ion adsorption

**Table 2** Calculated data for adsorption of As (III and V) ions on the $B_{12}N_{12}$ cage in the aqueous phase. The energies are in eV

| System | $\Delta H°$ | $\Delta G°$ | $Q_T$ (e) | $E_{HOMO}$ | $E_{LUMO}$ | $E_g$ | [a]$\Delta E_g$(%) |
|--------|------|------|------|------|------|------|------|
| $B_{12}N_{12}$ | – | – | – | −7.70 | −0.80 | 6.90 | – |
| a.3 | −7.9 | −7.7 | 1.70 | −10.03 | −6.76 | 3.27 | 52.6 |
| b.3 | −9.4 | −9.1 | 1.70 | −9.47 | −6.88 | 2.59 | 62.4 |
| a.5 | −50.6 | −50.3 | 3.42 | −11.78 | −10.83 | 0.95 | 86.2 |
| b.5 | −53.4 | −53.2 | 3.50 | −11.16 | −10.29 | 0.87 | 87.4 |

[a] The change of $E_g$ (HOMO/LUMO energy gap) of $B_{12}N_{12}$ upon the ion adsorption

As is seen from the DOSs in Fig. 2, the $E_g$ values are reduced from 6.84 eV to 0.81 and 1.18 eV in configurations **A.5** and **B.5**, respectively, revealing the point that their decrement amounts are much more than that of the $E_g$ upon the As (III) adsorptions.

Adsorption of As ions on the $B_{12}N_{12}$ in the aqueous phase

How does the solvent change the results of the As ions adsorption on the $B_{12}N_{12}$? To answer this question we have repeated all of the calculations in aqueous phase using PCM. Considering the optimized $B_{12}N_{12}$ cluster in the aqueous phase (aq) showed that the effects of the solvent on its structural and electronic properties were insignificant. As shown in Table 2, the $E_g$ value of the $B_{12}N_{12}$ (aq) is about 6.90 eV which is higher than that of the $B_{12}N_{12}$ (g) by about 0.06 eV. The range of vibrational frequencies is much affected by the solvent so that it is changed from 323.3 to 1427.5 $cm^{-1}$. $\Delta G°$ of solvation is calculated to be about −0.18 eV and $C_v$ of the cluster is increased from 51.36 to 51.77 $calmol^{-1}$ Kelvin.

The two obtained final optimized structures of the As (III)/$B_{12}N_{12}$ (aq) (configurations **a**.3 and **b**.3) and also those of the As (V)/$B_{12}N_{12}$ (aq) (configurations **a**.5 and **b**.5) are shown in Fig. 3. It can be found that the solvent significantly influences geometry parameters of the complexes. For example, comparing the configurations **B**.3 and **b**.3, it can be seen that in contrast to the case of **B**.3, the solvent considerably hinders the window creating in the surface of the cluster in the configuration **b**.3. This trend can also be observed in the other configurations. As shown in Table 2, the values of $\Delta H°$ and $\Delta G°$ for all of the adsorptions in the aqueous phase are less negative than those of corresponding values in the gas phase. The result indicates that the interaction between the As ion and the $B_{12}N_{12}$ cluster in the aqueous phase is much weaker than that in the gas phase. We think that increasing stabilization of the ions by the solvent results in decreasing reactivity. As is seen from the DOS plots in Fig. 3, the solvent also has considerable effect on the electronic properties of the complexes. For example, comparing the configurations **B**.5 and **b**.5, it can be seen that the energy levels of both HOMO and LUMO in the **B**.5 are much lower than those in **b**.5 and also the $E_g$ value of
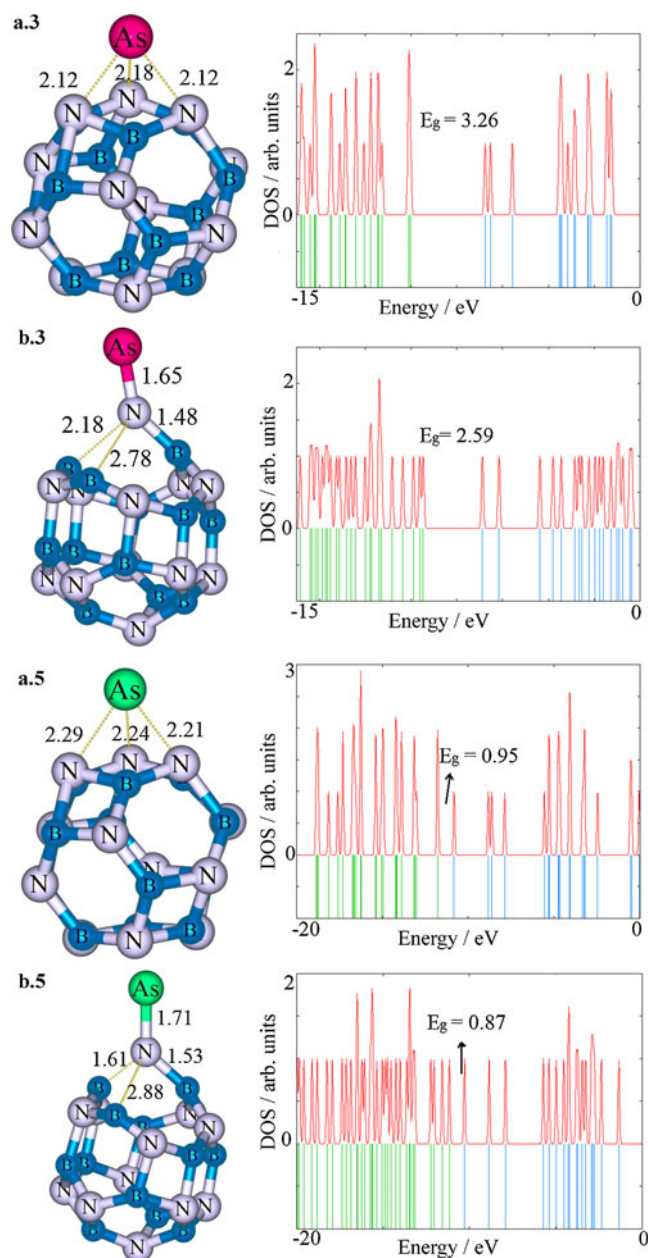


**Fig. 3** Geometry parameters of As/$B_{12}N_{12}$ complexes in aqueous phase and their density of state (DOS) plots. As (III) and (V) ions are shown in red and green, respectively. Distances are in Å

**B**.5 is higher than that of **b**.5 by about 0.31 eV. However, the influence of solvent on the electronic properties of these complexes does not follow a specific trend.

## Conclusions

Using DFT, we have investigated the adsorption of As (III and V) ions on the surface of $B_{12}N_{12}$ cage in vacuum and aqueous phase. It was found that these ions can be strongly chemisorbed on the surface of the cluster in both vacuum and aqueous phase with the Gibbs free energy change (at T= 298.18 K and P=1 atm) from −20.9 to −90.9 eV. The adsorptions significantly change the electronic properties of the cluster so that it transforms from a semi-insulator to a semiconductor. The solvent significantly influences the geometry parameters and electronic properties of the As/$B_{12}N_{12}$ complexes and the interaction between the components in the aqueous phase is noticeably weaker than that in vacuum.

## References

1. Korte NE, Fernando Q (1991) Crit Rev Environ Control 21:1–39
2. Satoshi E, Yansuko T, Yasuhiro K, Izumi N (2008) Environ Sci Technol 42:7152–7158
3. Pena ME, Korfiatis GP, Patel M, Lippincott L, Meng X (2005) Water Res 39:2327–2337
4. Kanel SR, Greneche JM, Choi H (2006) Environ Sci Technol 40:2045–2050
5. Wang Y, Reardon EJ (2001) Appl Geochem 16:531–539
6. Biswas K, Saha SK, Ghosh UC (2007) Ind Eng Chem Res 46:5346–5356
7. Hirsch A (1994) The chemistry of the fullerenes. Thieme, New York
8. Lal B (2007) J Mol Model 13:531–536
9. Chi M, Zhang Z, Han P, Fang X, Jia W, Dong H, Xu B (2008) J Mol Model 14:465–470
10. Oku T, Nishiwaki A, Narita I (2004) Sci Technol Adv Mater 5:635–638
11. Beheshtian J, Bagheri Z, Kamfiroozi M, Ahmadi A (2011) Microelectron J 42:1400–1403
12. Beheshtian J, Ahmadi A, Bagheri Z, Kamfiroozi M (2011) Struct Chem. doi:101007/s11224-012-9970-9
13. Beheshtian J, Kamfiroozi M, Bagheri Z, Ahmadi A (2012) Chin J Chem Phys 25:60–64
14. Schmidt M et al (1993) J Comput Chem 14:1347–1363
15. Bauschlicher CW (1995) Chem Phys Lett 246:40–44
16. Ahmadi A, Hadipour NL, Kamfiroozi M, Bagheri Z (2012) Sensors Actuators B Chem 161:1025–1029
17. Hernández Rosas J, Ramírez Gutiérrez R, Escobedo-Morales A, Chigo Anota E (2011) J Mol Model 17:1133–1139
18. Beheshtian J, Baei MT, Ahmadi A (2012) Surf Sci 606:981–985
19. Kaewruksa B, Ruangpornvisuti V (2012) J Mol Model 18:1447–1454
20. Ahmadi A, Beheshtian J, Hadipour N (2011) Struct Chem 22:183–188
21. Wang C, Xu S, Ye L, Lei W, Cui Y (2011) J Mol Model 17:1075–1080
22. Tomić S, Montanari B, Harrison NM (2008) Phys E 40:2125–2127
23. Li SS (2006) Semiconductor physical electronics, 2nd edn. Springer, Heidelberg